Bcl2L12-mediated inhibition of effector caspase-3 and caspase-7 via distinct mechanisms in glioblastoma

Alexander H. Stegh*, Santosh Kesari*†, John E. Mahoney‡, Harry T. Jenq§, Kristin L. Forloney*, Alexei Protopopov*‡, David N. Louis¶, Lynda Chin*‡‖, and Ronald A. DePinho*‡**††

*Department of Medical Oncology, and ‡Center for Applied Cancer Science of the Belfer Foundation Institute for Innovative Cancer Science, Dana–Farber Cancer Institute, Boston, MA 02115; †Center for Neuro-Oncology and Department of Neurology, Brigham and Women's Hospital, Boston, MA 02115; §Division of Health Sciences and Technology, Harvard Medical School and Massachusetts Institute of Technology, Boston, MA 02114; ¶Department of Pathology and Cancer Center, Massachusetts General Hospital and Harvard Medical School, Boston, MA 02114; and Departments of ‖Dermatology and **Medicine and Genetics, Harvard Medical School, Boston, MA 02115

Edited by William A. Weiss, University of California, San Francisco, CA, and accepted by the Editorial Board May 22, 2008 (received for review January 7, 2008)

Glioblastoma multiforme (GBM) is a highly aggressive brain cancer that is characterized by the paradoxical features of intense apoptosis resistance yet a marked propensity to undergo necrosis. Bcl2L12 (for Bcl2-Like12) is a nuclear and cytoplasmic oncoprotein that is universally overexpressed in primary GBM and functions to block postmitochondrial apoptosis signaling by neutralizing effector caspase-3 and caspase-7 maturation. This postmitochondrial block in apoptosis engenders the alternate cell fate of cellular necrosis, thus providing a molecular explanation for GBM's classical features. Whereas Bcl2L12-mediated neutralization of caspase-7 maturation involves physical interaction, the mechanism governing Bcl2L12-mediated inhibition of caspase-3 activity is not known. The nuclear localization of Bcl2L12 prompted expression profile studies of primary astrocytes engineered to overexpress Bcl2L12. The Bcl2L12 transcriptome revealed a striking induction of the small heat shock protein α-basic-crystallin (αB-crystallin/HspB5), a link reinforced by robust αB-crystallin expression in Bcl2L12-expressing orthotopic glioma and strong coexpression of αB-crystallin and Bcl2L12 proteins in human primary GBMs. On the functional level, enforced αB-crystallin or Bcl2L12 expression enhances orthotopic tumor growth. Conversely, RNAi-mediated knockdown of αB-crystallin in Bcl2L12-expressing astrocytes and glioma cell lines with high endogenous αB-crystallin showed enhanced apoptosis, yet decreased necrotic cell death with associated increased caspase-3 but not caspase-7 activation. Mirroring this specific effect on effector caspase-3 activation, αB-crystallin selectively binds procaspase-3 and its cleavage intermediates *in vitro* and *in vivo*. Thus, αB-crystallin is a Bcl2L12-induced oncoprotein that enables Bcl2L12 to block the activation of both effector caspases via distinct mechanisms, thereby contributing to GBM pathogenesis and its hallmark biological properties.

heat shock protein | apoptosis/necrosis balance | glial cells

Glioblastoma multiforme (GBM) is a highly aggressive brain cancer characterized by rapid tumor cell proliferation, intense apoptosis resistance, and marked necrosis, tumor biological features underlying its neurologically destructive course and its high lethality typically within 12–24 months of diagnosis. The mechanisms underlying GBM's intense apoptosis resistance and associated poor therapeutic responsiveness relate in part to the reinforcing activities of coactivated RTKs (1) and defective PTEN and p53 proteins (2, 3) and modulation of classical apoptosis regulators such as Bcl-2 family proteins (4–7), soluble decoy receptor 3 (DcR3) (8), APRIL (9), and PEA-15 (10–12).

In GBM oncogenomic studies, we identified and functionally characterized Bcl2L12 (for Bcl2-Like-12), a proline-rich and BH2 domain-containing protein that is robustly expressed in virtually all human primary GBM specimens (13). Enforced Bcl2L12 expression in primary cortical astrocytes conferred marked apoptosis resistance and engendered cellular necrosis through inhibition of effector caspase-3 and caspase-7 maturation downstream of mitochondria (13). The capacity of Bcl2L12 to block caspase-7 activation matched well with direct physical interaction *in vitro* and *in vivo* with the pro-caspase. The means through which Bcl2L12 inhibited caspase-3 was not defined and did not involve physical interaction between Bcl2L12 and caspase-3.

In this study, we sought to elucidate the mechanism of Bcl2L12-mediated neutralization of caspase-3. Transcriptome analyses of Bcl2L12-expressing astrocytic cultures revealed prominent up-regulation of αB-crystallin expression. The previously described capacity of recombinant αB-crystallin protein to inhibit caspase-3 activation in a cell-free system (14) prompted a detailed analysis of a potential Bcl2L12-αB-crystallin signaling axis in cultured astrocytes and glioma cell lines, orthotopic glioma xenotransplants, and primary GBM specimens. Gain- and loss-of-function assays and detailed biochemical studies in both normal and neoplastic glial model systems establish a pathway comprised of Bcl2L12–αB-crystallin–caspase-3 in the regulation of apoptosis and necrosis *in vitro* and *in vivo*. Together, these studies reveal the multifunctional nature of the Bcl2L12 oncoprotein, operating in both the cytoplasm and nucleus to effect survival signaling in gliomagenesis.

Results

Bcl2L12 Drives Up-Regulation of αB-Crystallin. The cytoplasmic presence of Bcl2L12 is consistent with its physical and inhibitory actions on caspase-7 (13). At the same time, abundant Bcl2L12 in the nucleoplasm prompted transcriptional profiling studies to assess whether the range of Bcl2L12's antiapoptotic activities might extend to more direct effects on gene expression. Strikingly, $Bcl2L12^{V5}$-expressing *Ink4a/Arf*-deficient cortical astrocytes showed marked up-regulation of αB-crystallin by micorarray, quantitative RT-PCR, and Western blot analyses [Fig. 1*A*, supporting information (SI) Table S1, and data not shown]. In contrast, αB-crystallin was unchanged in the context of Bcl-2 expression (Fig. 1*A*), suggesting that up-regulation of αB-crystallin is not a general function of Bcl-2 family proteins. The specific physiological link between Bcl2L12 and αB-crystallin is supported further by the inability of Bcl2L12 to influence expression of other apoptosis modulators including postmitochondrial caspases and their inhibitors and other members of the heat shock protein family such as Hsp70 and Hsp27 (Fig. 1*A* and Table S1). Table S2 provides a complete list of differentially expressed genes by 1.3-fold relative to empty vector controls.

Author contributions: A.H.S. and R.A.D. designed research; A.H.S., S.K., J.E.M., H.T.J., K.L.F., and A.P. performed research; A.H.S., S.K., J.E.M., A.P., D.N.L., and L.C. analyzed data; and A.H.S., L.C., and R.A.D. wrote the paper.

The authors declare no conflict of interest.

This article is a PNAS Direct Submission. W.A.W. is a guest editor invited by the Editorial Board.

††To whom correspondence should be addressed. E-mail: ron_depinho@dfci.harvard.edu.

This article contains supporting information online at www.pnas.org/cgi/content/full/0712034105/DCSupplemental.

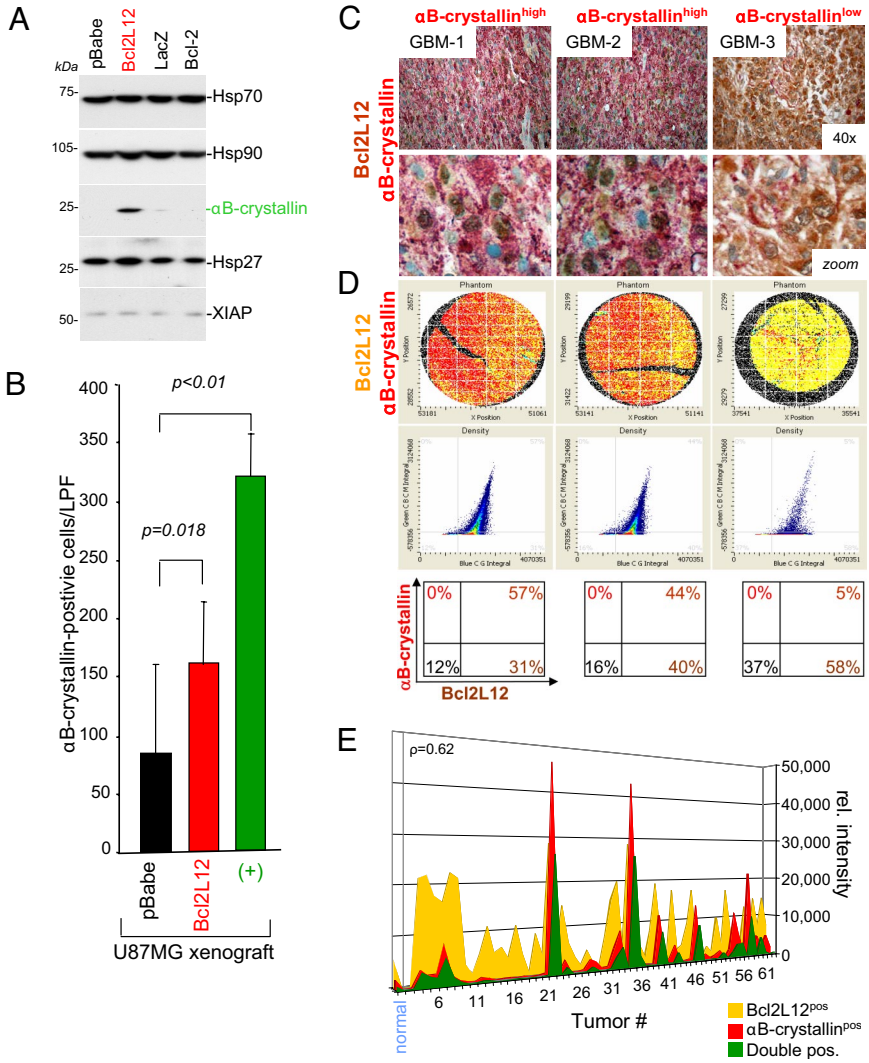

Fig. 1. Bcl2L12 up-regulates αB-crystallin protein levels *in vitro* and *in vivo*. (*A*) Western blot analysis of postmitochondrial apoptosis effectors in *Ink4a/Arf*$^{-/-}$ astrocytes ectopically expressing a pBabe control, Bcl2L12^{V5}, LacZ^{V5}, and Bcl-2. The migration positions of Hsp70, Hsp90, αB-crystallin, Hsp27, and XIAP are indicated. (*B*) Quantification of αB-crystallin positivity in U98MG xenograft tumor sections. A total of 10–15 low power fields (LPFs) per genotype were counted. Error bars represent SDs, and *P* values were calculated by using Student's *t* test. (*C*) Coexpression analysis of αB-crystallin and Bcl2L12 in primary human GBM. GBM cores were stained with a monoclonal anti-αB-crystallin antibody (red) and a polyclonal Bcl2L12 (anti-L12–2) antiserum (brown). Shown are three representative cores at ×40 magnifications. (*D*) Heat map (*Top*; yellow dots = Bcl2L12 positive; red dots = αB-crystallin positive) and density plot analyses (*Middle*) of Bcl2L12/αB-crystallin double stainings in three representative GBM cores shown in *C*. The percentages of Bcl2L12 and αB-crystallin-positive and -negative tumor cells are indicated (*Bottom*) with Bcl2L12 intensities plotted on the *x* axis and αB-crystallin intensities on the *y* axis. (*E*) Analysis of coexpression across 61 GBM cores in comparison with normal brain. Shown are intensity levels of Bcl2L12 (yellow), αB-crystallin (red), and levels of coexpression (green). Pearson correlation coefficient $\rho = 0.62$.

To assess whether Bcl2L12^{V5}-dependent up-regulation of αB-crystallin in cell culture is also operative in glioma cells *in vivo*, we examined αB-crystallin protein expression in intracranial xenotransplants derived from the well established U87MG human glioma model system. Bcl2L12^{V5} and EGFRvIII overexpression resulted in reduced survival of SCID mice after intracerebral orthotopic injection with ID_{50} values of 36 days (pBabe), 31 days (Bcl2L12^{V5}; $P = 0.043$ vs. pBabe), and 29 days (EGFRvIII; $P = 0.001$ vs. pBabe) (Fig. S1*A*). These Bcl2L12^{V5}-transduced tumors exhibited increased anti-αB-crystallin immunoreactivity relative to pBabe-transduced controls (Fig. 1*B* and Fig. S1*B*), whereas Hsp27 protein levels remain unchanged in Bcl2L12-driven and control xenografts (Fig. S1*B*). These experimental observations were consistent with quantitative RT-PCR (Fig. S2*A*) and immunohistochemistry (IHC) (Fig. S2*B*) analyses of primary human GBM. Specifically, using a well characterized highly specific anti-αB-crystallin mAb, we detected strong αB-crystallin signal in 41 of 47 primary and 3 of 6 secondary GBM samples (Fig. S2*B* for representative cores). αB-crystallin staining is restricted to tumor cells without demonstrable positivity in endothelial cells of the tumor vasculature (Fig. S2*B*).

Our previous work established that Bcl2L12 is robustly expressed in >90% of human primary GBM specimens by IHC-tissue microarray (TMA) analysis (13). To examine further possible Bcl2L12-αB-crystallin coexpression, we used iCys laser scanning cytometry technology in IHC-TMA analyses (see *SI Methods* for detailed staining protocol and analysis methodology). Triply stained for Bcl2L12 [diaminobenzidine (DAB), brown], αB-crystallin (FastRed), and hematoxylin, TMA sections were scanned with three lasers in distinct wavelength channels, demonstrating the coexpression of both proteins (Fig. 1*C*). Heat maps and density plots of representative primary GBM cores with high and low αB-crystallin expression revealed that all αB-crystallin overexpressing tumor cells are also positive for Bcl2L12 (Fig. 1*D*). Analysis of Bcl2L12 and αB-crystallin distribution across 61 GBM cores revealed significant correlation between Bcl2L12 and αB-crystallin expression ($\rho = 0.62$; Fig. 1*E*). Coexpression of both proteins was confirmed further by intensity profiles of single tumor cells, documenting that highest Bcl2L12 expression coincided with highest αB-crystallin expression (Fig. S3). Together, these multilevel expression studies suggest an association between Bcl2L12 and αB-crystallin expression in primary and transformed glial cells *in vitro* and in experimental models and primary tumors *in vivo*.

αB-Crystallin Is Antiapoptotic and Protumorigenic in Human Glioma Cells *in Vitro* and *in Vivo*. To explore the cancer biological relevance of αB-crystallin, we monitored apoptosis signaling upon knockdown of αB-crystallin or other apoptosis inhibitors operating at the mitochondrial (e.g., Bcl-2) or postmitochondrial levels (e.g., Bcl2L12 and XIAP). We selected LN235 glioma cells on the basis of high endogenous Bcl2L12 and αB-crystallin expression. After verification of knockdown for the specific proteins (Fig. 2*A*),

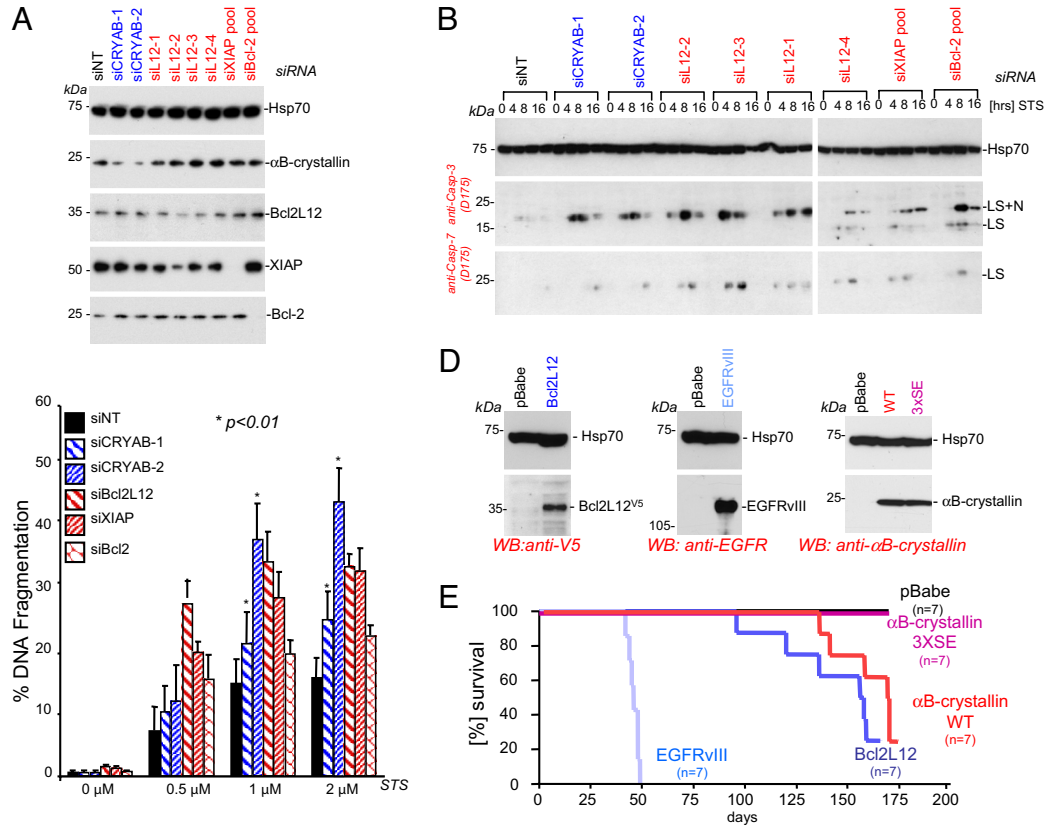

Fig. 2. αB-crystallin is a potent antiapoptotic protein in human glioma cells. (*A*) LN235 cells were transfected with RNAi oligonucleotides (each 100 nM) targeting αB-crystallin (siCRYAB-1 and siCRYAB-2), Bcl2L12 (siL12–1 to siL12–4), XIAP, and Bcl-2 (siRNA pools) and subjected to Western blot analysis to assess levels of protein knockdown. The migration positions of αB-crystallin, Bcl2L12, XIAP, and Bcl-2 are indicated. Hsp70 is shown as a loading control. (*B*) LN235 cells transfected with the indicated RNAi oligonucleotides were treated with STS (2 μM) for 0, 4, 8, and 16 h and subjected to Western blot analysis to assess effector caspase activation status. The migration positions of active caspase-3 and active caspase-7 species are indicated. Hsp70 protein levels are shown as a loading control. (*C*) LN235 transfectants were treated with the indicated doses of STS for 24 h, and DNA fragmentation was assessed by quantification of subG1 DNA peaks. Mean values of three to four independent experiments are shown with error bars representing SDs, and *P* values were calculated by using Student's *t* test. (*D*) Western blot analysis of LN443 cells retrovirally transfected with $Bcl2L12^{V5}$, EGFRvIII, αB-crystallin WT, and 3XSE point mutants. The migration positions of Bcl2L12, EGFRvIII, αB-crystallin and Hsp70 (loading control) are indicated. (*E*) Kaplan-Meier curves of SCID animals intracranially injected with LN443 cells retrovirally transduced with pBabe control, αB-crystallin WT, and 3XSE, $Bcl2L12^{V5}$ and EGFRvIII. ID_{50} and *P* values (vs. pBabe): WT (167 days, $P = 0.046$), 3XSE (not determined), Bcl2L12 (157 days, $P = 0.0042$), EGFRvIII (46 days, $P < 0.001$). *P* values were calculated by using logrank test.

Western blot analysis of effector caspase activation profiles revealed a predominant increase in active caspase-3 species with marginal effect on caspase-7 activation upon αB-crystallin knockdown compared with nontargeting control (siNT) (Fig. 2*B*). In contrast, knockdown of Bcl2L12 or to a lesser extent of XIAP and Bcl-2 resulted in enhanced of caspase-3 activation and caspase-7 activation (Fig. 2*B*; see Fig. S4 for a second representative experiment using a siRNA pool for Bcl2L12 knockdown) that translated into increased DNA fragmentation levels (Fig. 2*C*). Enhanced DNA fragmentation upon αB-crystallin knockdown was also observed in U373MG cells, which also show abundant Bcl2L12 and αB-crystallin expression (data not shown).

Next, the *in vivo* oncogenic potential of αB-crystallin, Bcl2L12, and EGFRvIII was assessed in the nontumorigenic human glioma cell line LN443, which expresses relatively low levels of endogenous Bcl2L12 and αB-crystallin (Fig. 2*D* and data not shown). Because of the well described effects of αB-crystallin phosphorylation on its diverse biological activities in mammary epithelial cells (14–17), we also examined whether the nonfunctional phosphorylation-deficient (S19E/S45E/S59E, labeled 3XSE) mutant affected the gliomagenic potential of LN443 cells *in vivo*. Expression levels of αB-crystallin proteins were comparable to endogenous αB-crystallin found in glioma cell lines, such as LN235, U373MG, and LN215 (data not shown). Orthotopic implantation of LN443 cells with enforced expression of αB-crystallin, Bcl2L12, or EGFRvIII resulted in tumor formation and reduced survival, whereas pBabe- or 3XSE-transduced LN443 cells failed to produce tumors (Fig. 2 *D* and *E*). Thus, enforced αB-crystallin expression in human glioma cells enhances tumorigenic potential, further validating αB-crystallin as an oncoprotein in GBM.

αB-Crystallin Colocalizes With and Binds to Caspase-3 *in Vitro and in Vivo*. The prominent effects of αB-crystallin on caspase-3 activity prompted detailed localization and immunoprecipitation studies of αB-crystallin and caspase-3 species in cortical *Ink4a/Arf*-deficient astrocytes. First, subcellular fractionation experiments reveal co-compartmentalization of αB-crystallin and caspase-3 species in the cytosol of Bcl2L12-expressing astrocytes (Fig. 3*A*). Second, GST pull-down assays show specific interaction of recombinant αB-crystallin protein with pro-caspase-3 and its cleavage intermediates (Fig. 3*B*, lanes 11 and 12), but not with caspase-7 or caspase-9 (Fig. 3*B*, lanes 9 and 10). Third, coimmunoprecipitation assays show selective binding of caspase-3, but not caspase-7, to αB-crystallin in untreated and, to a lesser extent, in apoptosis-primed Bcl2L12-expressing astrocytes (Fig. 3*C*). Finally, deconvolution immunofluorescence microscopy revealed partial colocalization of αB-crystallin with pro-caspase-3 and a more extensive colocalization with active caspase-3 in the cytosol of apoptosis-primed cells (Fig. S5). Thus, we conclude that αB-crystallin binds caspase-3 in astrocytes on an endogenous protein level.

αB-Crystallin Knockdown Sensitizes Bcl2L12-Expressing Astrocytes Toward Apoptosis in Association with Increased Effector Caspase Activity. To further assess the functional relevance of αB-crystallin in relation to Bcl2L12's cell death activities, we screened four individual siRNA oligonucleotides to identify two with significant knockdown of αB-crystallin protein levels in $Bcl2L12^{V5}$-expressing astrocytes (Fig. 4*A*, siCRYAB-1 and siCRYAB-2). Using these two siRNAs, we examined the effect of αB-crystallin knockdown on caspase-3 and caspase-7 activation in response to staurosporine (STS) in control or Bcl2L12-expressing *Ink4a/Arf*-deficient astro-

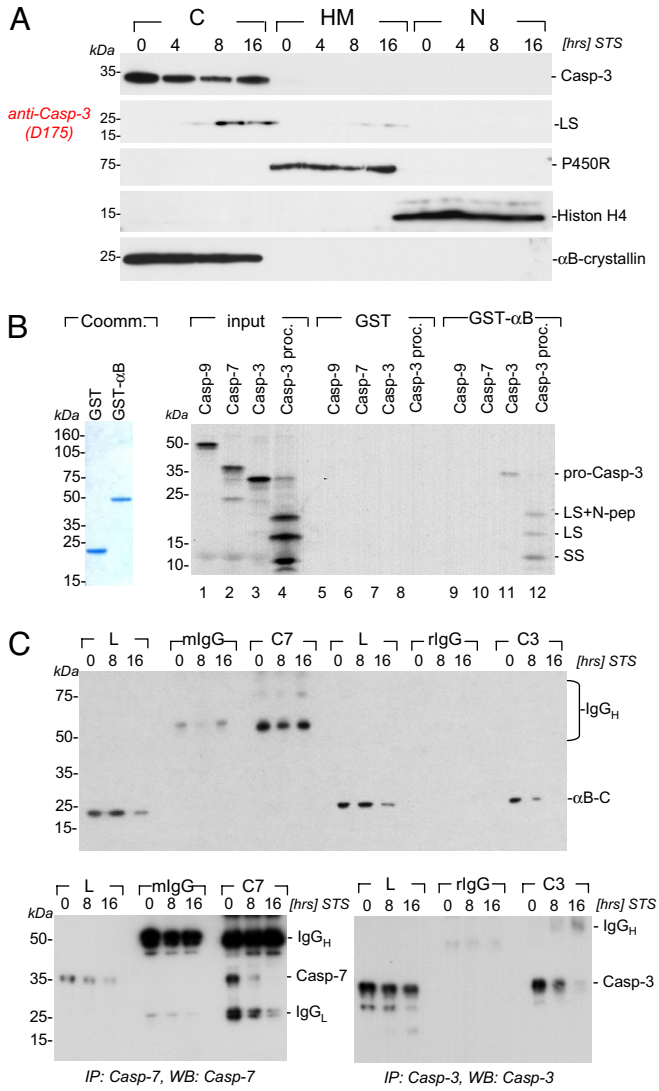

Fig. 3. αB-crystallin cocompartmentalizes with and selectively binds to the caspase-3 zymogen and its cleavage intermediates. (*A*) Bcl2L12^{V5}-expressing *Ink4a/Arf*-deficient astrocytes were treated with STS (1 μM) for the indicated periods of time, and cytosolic (C), heavy membranous (HM), and nuclear (N) compartments were prepared as described in *Methods*. Besides αB-crystallin, pro- and active caspase-3 species, the migration positions of cytochrome *c* P450 reductase (P450R), histon H4 and caspase-3 as membrane, nuclear and cytosolic markers are indicated. (*B*) Affinity-purified GST and GST-αB-crystallin fusion proteins (Coommassie-stained gel for purity assessment) were used in GST pull-down experiments to assess for αB-crystallin:caspase complex formation. GST or GST-αB-crystallin proteins were incubated with [^{35}S]labeled *in vitro*-translated pro-caspase-9 (Casp-9), pro-caspase-7 (Casp-7), pro-caspase-3 (Casp-3), and pro-caspase-3 preincubated with 20 ng of active caspase-8 (Casp-3$^{proc.}$) to induce proteolytic processing of the zymogen. A representative autoradiogram with the migration positions of the caspase-3 pro-enzyme and its active subunits (SS, small subunit; LS, large subunit; LS+N pep, large subunit plus N-terminal peptide) is shown. (*C*) Bcl2L12^{V5}-expressing astrocytes were treated with STS (1 μM) for the indicated periods of time, lysed, and subjected to immunoprecipitation by using monoclonal mouse anti-caspase-7 and rabbit anti-caspase-3 antibodies followed by Western blot analysis under nonreducing conditions for αB-crystallin, caspase-3, and caspase-7. The migration positions of IgG and αB-crystallin, caspase-7, and caspase-3 are indicated.

cytes. As previously reported, Bcl2L12 expression inhibited both caspase-3 and caspase-7 activation (compare siNT time courses in pBabe vs. Bcl2L12; Fig. 4*B*). Knockdown of αB-crystallin protein in Bcl2L12-expressing astrocytes resulted in specific restoration of caspase-3 activation in response to STS treatment, but had no effect on caspase-7. This translated into sensitization to apoptosis as reflected by increased DNA fragmentation (Fig. 4*C*). Because of mitochondrial dysfunction, yet blockage of effector caspase activity, Bcl2L12-expressing *Ink4a/Arf*-deficient astrocytes showed marked enhancement of necrotic cell death (13). Expectedly, αB-crystallin knockdown reduced necrogenesis as evidenced by a detailed analysis of cellular morphology using transmission electron microscopy (TEM) (Fig. 4 *D* and *E*) as a consequence of the aforementioned increase in caspase-3-mediated apoptotic cell death.

Discussion

In this study, we provide functional and biochemical evidence that αB-crystallin is a Bcl2L12-induced caspase-3 inhibitor in normal and transformed glial cells. Mechanistically, αB-crystallin specifically interacts with and inhibits caspase-3, but not caspase-7, complementing the impact of Bcl2L12 as a direct caspase-7-binding and inhibitory protein on effector caspase activation. The glioma relevance of the Bcl2L12-αB-crystallin connection is supported by their coexpression in primary GBM samples and their capacity to inhibit apoptosis and enhance tumorigenesis in physiologically relevant systems. These expression and activity profiles support the view that Bcl2L12 and αB-crystallin are gliomagenic oncoproteins that cooperate to promote apoptosis resistance in GBM.

αB-crystallin is a small heat shock protein with known apoptosis regulatory activity as evidenced by its capacity to inhibit programmed cell death associated with death receptor ligation, oxidative stress, chemotherapy, and growth factor withdrawal (14–16, 18). Cell-free assays and overexpression studies demonstrated binding to and inhibition of partially processed caspase-3 (14–16). Additionally, αB-crystallin is overexpressed in several cancers, including malignant glioma (19–21). These previous observations, together with findings of this study in astrocytes and gliomas, strongly support an important oncogenic role for αB-crystallin as a downstream effector of Bcl2L12 in cell death signaling in GBM.

In astrocytes, RNAi-mediated depletion of caspase-7 promoted a pronecrotic response (13) and DNA fragmentation was affected by caspase-3 and caspase-7 knockdown (data not shown). In addition, caspase-3 and caspase-7 are activated in parallel, not sequentially downstream of mitochondria in cortical astrocytes (ref. 22 and data not shown). These experimental observations indicate important roles for both effector caspases in apoptosis signaling in astrocytes and, therefore, provide a mechanistic rational for coexpression of Bcl2L12 and αB-crystallin in gliomagenesis. In addition, it is intriguing that astrocytes possess a mitochondrial physiology that is somewhat distinct from other cell types. Previous studies have demonstrated that, under normal culture conditions, astrocyte mitochondria exhibit elevated basal mitochondrial potential (23) and oxygen/glucose deprivation fails to induce mitochondrial dysfunction and consequently apoptosis (24). Significant glycogen reservoirs and inducible glycolysis may guarantee sustained ATP levels that lead to robust steady-state protection of mitochondrial membranes in astrocytes, pointing to effector caspase activation rather than mitochondrial membrane disintegration as a central target for apoptosis inhibition.

Aberrant activation of the PI3K pathway plays a prominent role in GBM pathogenesis. It can be targeted at the level of RTK activation and downstream PI3K signaling, including AKT amplification and foremost loss of the PI3K antagonist PTEN, which is inactivated by loss of heterozygosity in 70% and mutation in 40% of primary GBMs (25). Notably, ectopic expression of αB-crystallin was shown to enhance AKT and ERK1/2 activation, resulting in enhanced proliferative capacity of mammary epithelial cells (17). It is tempting to speculate that Bcl2L12-induced αB-crystallin upregulation acts cooperatively with PI3K pathway hyperactivation to promote glial cell survival and proliferation, suggesting dual roles for the Bcl2L12–αB-crystallin axis in both apoptosis and mitogenic signaling.

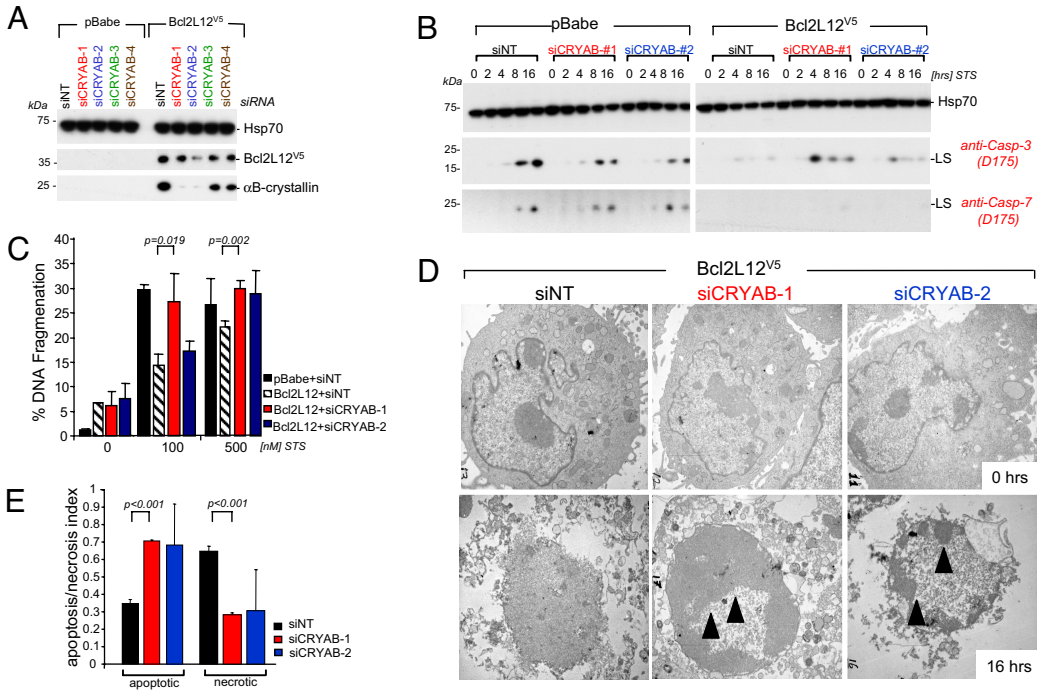

Fig. 4. RNAi-mediated knockdown of αB-crystallin in Bcl2L12-expressing astrocytes enhances apoptotic and decreases necrotic cell death. (*A*) Western blot analysis for αB-crystallin in pBabe- and Bcl2L12-expressing astrocytes transfected with RNAi oligonucleotides (50 nM; siNT, nontargeting oligonucleotide; siCRYAB-1 to siCRYAB-4, αB-crystallin-specific oligonucleotides). Hsp70 is shown as a loading control. (*B*) pBabe- and Bcl2L12-expressing astrocytes transfected with siNT and αB-crystallin-targeting RNAi oligonucleotides were treated with STS (0.5 μM) for the indicated periods of time and subsequently subjected to Western blot analysis using antibodies specific for cleaved caspase-3 and caspase-7 species. The migration positions of the large subunits (LS) are indicated. Hsp70 is shown as a loading control. (*C*) pBabe- and Bcl2L12-expressing astrocytes transfected with siRNA oligonucleotides were treated with the indicated doses of STS for 24 h, and DNA fragmentation was assessed by FACS-based quantification of subdiploid DNA content. The means of three independent experiments are shown. Error bars represent SDs, and *P* values were calculated by using Student's *t* test. (*D*) TEM of Bcl2L12-expressing astrocytes transfected with siNT or siCRYAB-1, siCRYAB-2 oligonucleotides. Shown are representative micrographs of untreated and STS-treated cells (1 μM). (Bar: 1 μm). Filled arrowheads point to condensed chromatin as a hallmark characteristic of apoptotic cells. Note the absence of chromatin condensation in siNT-transfected Bcl2L12-expressing astrocytes, and the occurrence of such structures within the nucleus of siCRYAB-treated cells. (*E*) Quantification of apoptotic and necrotic cells as determined by the absence or presence of plasma membrane integrity and chromatin condensation of TEM micrographs. Error bars depict SDs, and *P* values were calculated by using Student's *t* test.

Based on (*i*) the importance of postmitochondrial caspase activation for apoptosis propagation and execution in glial cells, (*ii*) the selective effects of αB-crystallin knockdown on caspase-3 activation (Figs. 2*B* and 4*B*), (*iii*) the specific interaction with pro and active caspase-3 species on endogenous protein levels (Fig. 3), and (*iv*) the selective inhibition of caspase-3, but not caspase-7, activation by recombinant αB-crystallin in a cell-free dATP/cytc caspase-activation assay (14), we propose that IAP-like caspase-3 neutralization either by preventing the proteolytic processing of the zymogen and/or by direct modulation of the active enzyme is a major route through which αB-crystallin exerts its antiapoptotic activity. On the basis of other studies, it is possible that additional mechanisms, such as interaction with Bcl-x_S, Bax and p53 to block their translocation to mitochondria (26, 27) and antioxidant activities possibly relating to up-regulation of glucose-6-phosphate dehydrogenase (28,29), might further contribute to the antiapoptotic profile of αB-crystallin and will require additional study in normal and transformed glial cells.

The convergence of Bcl2L12 and αB-crystallin in the inhibition of effector caspase signaling, the frequent and robust overexpression of αB-crystallin and Bcl2L12 in GBM, and the proven efficacy of antagonizing effector caspase activity in tumor cells (30) support the development of targeted drugs to block the actions of Bcl2L12/αB-crystallin on effector caspases. The findings of this study predict that enablement of effector caspase function will enhance the responsiveness of GBM to proapoptotic agents such as chemo and radiation therapy.

Methods

Affymetrix Expression Profiling. Total RNA was isolated from subconfluent *Ink4a/Arf*-deficient astrocytes stably expressing a pBabe control or Bcl2L12^{V5} (for retroviral transduction of astrocytes see ref. 13) by using TRIzol (Invitrogen) and an RNeasy mini kit (Qiagen). Gene expression profiling was performed on the Affymetrix M430A platform with three independent total RNA preparations. Raw gene expression was analyzed by dChip software (31).

Subcellular Fractionation. Subconfluent Bcl2L12^{V5}-expressing astrocytic cultures were stimulated with STS (1 μM) for the indicated periods of time, and cytosolic, nuclear, and membrane fractions were prepared by using the Protean Kit (Calbiochem) according to the manufacturer's instructions followed by Western blot analysis using caspase-3, active caspase-3, cytochrome P450 reductase, and histone H4 antibodies (see below).

siRNA Transfection. Subconfluent glioma cells or astrocytes were transfected with siRNA oligonucleotides (Dharmacon) (siRNA nontargeting control; D-001210-01-20), mouse-specific siCRYAB-1 (J-043201-09), siCRYAB-2 (J-043201-10), siCRYAB-3 (J-043201-11), siCRYAB-4 (J-043201-12), human-specific siCRYAB-1 (J-009743-09), siCRYAB-2 (J-009743-10), siBcl2L12–1 (J-017207-05), siBcl2L12–2 (J-017207-06), siBcl2L12–3 (J-017207-07), siBcl2L12–4 (J-017207-08), siBcl2 (L-003307-00), and siXIAP (L-004098-00) at a concentration of 50–100 nM by using Oligofectamine (Invitrogen). Cells were treated with STS 48 h after transfection and assayed for DNA fragmentation and caspase maturation.

***In Vivo* Xenograft Studies.** U87MG (1×10^5 cells) and LN443 transfectants (1×10^6 cells) were injected intracranially into SCID mice ($n = 7$ for each transfectant). Cells were suspended in HBSS, injected through a burr hole (0.5 mm anterior and 2.0 mm lateral to the Bregma) into the skull of 6-week-old SCID mice that were anesthetized with ketamine (60 mg/kg) and xylazine (7.5 mg/kg), and placed in the stereotactic frame by using ear bars. Cells were injected (total volume 2 μl) at a depth of 3.0 mm from the surface of the brain. The scalp was closed with 5.0 silk suture. Animals were followed daily for development of neurological deficits. For pathological analyses, all animals were deeply anesthetized, and their brains were fixed by intracardiac perfusion with 4% paraformaldehyde followed by an additional 12 h of immersion fixation.

Analysis of DNA Fragmentation. Cells were treated with STS (Sigma; 0–2 μM), trypsinized, washed with PBS, and subsequently resuspended in Nicoletti buffer (0.1% Tx-100, 0.1% Na-Citrate, 50 μg/ml propidium iodide). Nuclei were analyzed by FACS to quantify sub-G_1 DNA content.

GST-αB-Crystallin Protein Preparation, GST Pull-Down Experiments, Immunoprecipitations, and Western Blot Analysis. GST-αB-crystallin was constructed by PCR amplification of the αB-crystallin cDNA (provided by V. Cryns, Northwestern University, Chicago) and cloning of the PCR fragment into pGex4T1. For isolation of recombinant GST and GST-αB-crystallin proteins, BL21 bacteria (A_{600nm} 0.6–0.8) were induced with isopropyl β-D-thiogalactoside (Sigma) for 4 h at a concentration of 1 μM. Cells were washed once with STE buffer [10 mM Tris (pH 8.0), 150 mM NaCl, 1 mM EDTA], lysed, and sonicated in NETN buffer with 1 mM DTT and 5% Sarcosyl. Lysates were cleared by centrifugation (5,000 × *g*) and incubated with GSH-Sepharose 4B (Amersham) for 2 h at 4°C. Beads were washed five times with NETN buffer and resuspended in IP buffer [0.2% Nonidet P-40, 20 mM Hepes, 142 mM KCl, 1 mM EDTA, complete protease inhibitor mixture (Roche)].

For pull-down experiments, GST fusion proteins were preincubated in IP buffer containing 0.1% BSA to block unspecific binding and subsequently incubated with *in vitro*-translated, [^{35}S]methionine-labeled proteins overnight at 4°C in IP buffer. Subsequently, beads were washed five times with IP buffer, and associated proteins were analyzed by 4–12% SDS/PAGE followed by autoradiography. For *in vitro* processing of caspase-3, 20 ng of recombinant active caspase-8 (BD Biosciences) was added to [^{35}S]radiolabeled caspase-3 for 1 h at 37°C in assay buffer (20 mM Hepes-KOH, 100 mM NaCl, 0,1% CHAPS, 10% sucrose, 1 mM DTT). For immunoprecipitations using monoclonal anti-caspase-3 (Cell Signaling) and anti-caspase-7 antibodies (BD Biosciences), postnuclear supernatants were incubated with mIgG control antibodies coupled to Protein A/G-Sepharose 4B beads (Sigma) and subsequently with anti-caspase-7 and caspased-3 antibodies (1 μg) overnight. Immunoprecipitates were washed three times with IP buffer and subjected to 4–12% SDS/PAGE followed by Western blot analysis for αB-crystallin.

For all Western blot analyses, proteins were separated by 4–12% SDS/PAGE, transferred to Hybond PVDF membranes (Amersham), blocked with 5% milk in PBS with 0.05% Tween 20 (PBS/Tween) for 1 h, washed with PBS/Tween, and incubated with the following antibodies: anti-cytochrome P450 reductase (1:1,000; Santa Cruz Biotechnologies), anti-caspase-3, anti-caspase-7 (1:1,000; BD Biosciences), anti-cleaved caspase-3 (1:1,000; Calbiochem), anti-cleaved capase-7 (1:1,000; Calbiochem), anti-Hsp70 and Hsp90 (1:4,000; BD Pharmingen), anti-L12–1 (1 μg/ml), anti-Bcl2 (1:1,000; BD Biosciences), EGFR (1:1,000; Santa Cruz Biotechnologies), anti-XIAP (1:1,000; BD Biosciences), anti-Hsp27 (1:1,000; Santa Cruz Biotechnologies), anti-V5 (1:5,000; Invitrogen), anti-αB-crystallin (1:4,000; Stressgen), and anti-Histone H4 (1:4,000; Upstate). The blots were washed with PBS/Tween and developed with goat anti-rabbit IgG (1:10,000) or goat anti-mouse antibodies (1:10,000) (Pierce) in 5% milk PBS/Tween. After washing with PBS/Tween, the blots were developed with the Lumigen PS3 kit (Amersham) following the manufacturer's protocol.

ACKNOWLEDGMENTS. We thank Dr. Vincent Cryns for providing the αB-crystallin WT and 3XSE cDNAs, Drs. Junying Yuan (Harvard Medical School) and Emad Alnemri (Kimmel Cancer Center, Philadelphia) for the caspase-3, caspase-7, and caspase-9 expression plasmids, Drs. Frank Furnari (University of California, San Diego) and Webster K. Cavenee (University of California, San Diego) for glioma cell lines, and Elizabeth Benecchi of the electron microscopy facility of Harvard Medical School for assistance with the TEM studies. A.H.S. was supported by a Claudia-Adams Barr Award and National Institutes of Health Grant K99CA129172. S.K. was supported by National Institutes of Health Grant K08CA124804 and a Sontag Foundation Distinguished Scientist Award. This work was also supported by National Institutes of Health Grants PO1 CA95616 (to R.A.D., D.N.L., and L.C.) RO1 CA099041 (to L.C.), and RO1 CA57683 (to D.N.L.) and awards from the Bernard A. and Wendy J. Goldhirsh Foundation and the Christopher Elliot Foundation (to R.A.D. and L.C.).

1. Stommel JM, *et al.* (2007) Coactivation of receptor tyrosine kinases affects the response of tumor cells to targeted therapies. *Science* 318:287-290.
2. Furnari FB, *et al.* (2007) Malignant astrocytic glioma: Genetics, biology, and paths to treatment. *Genes Dev* 21:2683-2710.
3. Louis DN (2006) Molecular pathology of malignant gliomas. *Annu Rev Pathol* 1:97-117.
4. Jiang Z, Zheng X, Rich KM (2003) Down-regulation of Bcl-2 and Bcl-xL expression with bispecific antisense treatment in glioblastoma cell lines induce cell death. *J Neurochem* 84:273-281.
5. Julien T, *et al.* (2000) Antisense-mediated inhibition of the bcl-2 gene induces apoptosis in human malignant glioma. *Surg Neurol* 53:360-369.
6. Krajewski S, *et al.* (1997) Immunohistochemical analysis of Bcl-2, Bcl-X, Mcl-1, and Bax in tumors of central and peripheral nervous system origin. *Am J Pathol* 150:805-814.
7. Strik H, *et al.* (1999) BCL-2 family protein expression in initial and recurrent glioblastomas: Modulation by radiochemotherapy. *J Neurol Neurosurg Psychiatry* 67:763-768.
8. Roth W, *et al.* (2001) Soluble decoy receptor 3 is expressed by malignant gliomas and suppresses CD95 ligand-induced apoptosis and chemotaxis. *Cancer Res* 61:2759-2765.
9. Roth W, *et al.* (2001) APRIL, a new member of the tumor necrosis factor family, modulates death ligand-induced apoptosis. *Cell Death Differ* 8:403-410.
10. Condorelli G, *et al.* (1999) PED/PEA-15: An antiapoptotic molecule that regulates FAS/TNFR1-induced apoptosis. *Oncogene* 18:4409-4415.
11. Ramos JW, *et al.* (2000) Death effector domain protein PEA-15 potentiates Ras activation of extracellular signal receptor-activated kinase by an adhesion-independent mechanism. *Mol Biol Cell* 11:2863-2872.
12. Eckert A, *et al.* (2008) The PEA-15/PED protein protects glioblastoma cells from glucose deprivation-induced apoptosis via the ERK/MAP kinase pathway. *Oncogene* 27:1155-1166.
13. Stegh AH, *et al.* (2007) Bcl2L12 inhibits postmitochondrial apoptosis signaling in glioblastoma. *Genes Dev* 21:98-111.
14. Kamradt MC, Chen F, Cryns VL (2001) The small heat shock protein αB-crystallin negatively regulates cytochrome *c*- and caspase-8-dependent activation of caspase-3 by inhibiting its autoproteolytic maturation. *J Biol Chem* 276:16059-16063.
15. Kamradt MC, Chen F, Sam S, Cryns VL (2002) The small heat shock protein αB-crystallin negatively regulates apoptosis during myogenic differentiation by inhibiting caspase-3 activation. *J Biol Chem* 277:38731-38736.
16. Kamradt MC, *et al.* (2005) The small heat shock protein αB-crystallin is a novel inhibitor of TRAIL-induced apoptosis that suppresses the activation of caspase-3. *J Biol Chem* 280:11059-11066.
17. Moyano JV, *et al.* (2006) αB-crystallin is a novel oncoprotein that predicts poor clinical outcome in breast cancer. *J Clin Invest* 116:261-270.
18. Mehlen P, *et al.* (1995) Constitutive expression of human hsp27, *Drosophila* hsp27, or human αB-crystallin confers resistance to TNF- and oxidative stress-induced cytotoxicity in stably transfected murine L929 fibroblasts. *J Immunol* 154:363-374.
19. Aoyama A, Frohli E, Schafer R, Klemenz R (1993) αB-crystallin expression in mouse NIH 3T3 fibroblasts: Glucocorticoid responsiveness and involvement in thermal protection. *Mol Cell Biol* 13:1824-1835.
20. Hitotsumatsu T, Iwaki T, Fukui M, Tateishi J (1996) Distinctive immunohistochemical profiles of small heat shock proteins (heat shock protein 27 and αB-crystallin) in human brain tumors. *Cancer* 77:352-361.
21. Kato S, Hirano A, Kato M, Herz F, Ohama E (1993) Comparative study on the expression of stress-response protein (srp) 72, srp 27, αB-crystallin and ubiquitin in brain tumors: An immunohistochemical investigation. *Neuropathol Appl Neurobiol* 19:436-442.
22. Slee EA, *et al.* (1999) Ordering the cytochrome *c*-initiated caspase cascade: hierarchical activation of caspases-2, -3, -6, -7, -8, and -10 in a caspase-9-dependent manner. *J Cell Biol* 144:281-292.
23. Diaz G, *et al.* (1999) Subcellular heterogeneity of mitochondrial membrane potential: Relationship with organelle distribution and intercellular contacts in normal, hypoxic, and apoptotic cells. *J Cell Sci* 112:1077-1084.
24. Almeida A, Delgado-Esteban M, Bolanos JP, Medina JM (2002) Oxygen and glucose deprivation induces mitochondrial dysfunction and oxidative stress in neurones but not in astrocytes in primary culture. *J Neurochem* 81:207-217.
25. Li J, *et al.* (1997) PTEN, a putative protein tyrosine phosphatase gene mutated in human brain, breast, and prostate cancer. *Science* 275:1943-1947.
26. Liu S, Li J, Tao Y, Xiao X (2007) Small heat shock protein αB-crystallin binds to p53 to sequester its translocation to mitochondria during hydrogen peroxide-induced apoptosis. *Biochem Biophys Res Commun* 354:109-114.
27. Mao YW, Liu JP, Xiang H, Li DW (2004) Human αA- and αB-crystallins bind to Bax and Bcl-X(S) to sequester their translocation during staurosporine-induced apoptosis. *Cell Death Differ* 11:512-526.
28. Mehlen P, Kretz-Remy C, Preville X, Arrigo AP (1996) Human hsp27, *Drosophila* hsp27, and human αB-crystallin expression-mediated increase in glutathione is essential for the protective activity of these proteins against TNF-α-induced cell death. *EMBO J* 15:2695-26706.
29. Preville X, *et al.* (1999) Mammalian small stress proteins protect against oxidative stress through their ability to increase glucose-6-phosphate dehydrogenase activity and by maintaining optimal cellular detoxifying machinery. *Exp Cell Res* 247: 61-78.
30. Schimmer AD, *et al.* (2004) Small-molecule antagonists of apoptosis suppressor XIAP exhibit broad antitumor activity. *Cancer Cell* 5:25-35.
31. Li C, Hung Wong W (2001) Model-based analysis of oligonucleotide arrays: Model validation, design issues, and standard error application. *Genome Biol* 2:RESEARCH0032.